The Effect of Solution Concentration on the Electrochemical Behaviour of AISI 321 Stainless Steel in Sulfuric Solutions

A. Fattah-alhosseini[1]*, H. Farahani[2] and O. Imantalab[3]

Faculty of Engineering, Bu-Ali Sina University, Hamedan 65178-38695, Iran

Abstract

The semiconductor properties of passive films formed on AISI 321 stainless steel (AISI 321) in six acidic solutions under open circuit potential (OCP) conditions were evaluated by potentiodynamic polarization, Mott–Schottky analysis and electrochemical impedance spectroscopy (EIS). Mott–Schottky analysis revealed that the passive films behaved as n-type and p-type semiconductors at potentials below and above the flat band potential, respectively. Also, Mott–Schottky analysis indicated that the donor and acceptor densities were in the range 10^{21} cm^{-3} and increased with solution concentration. EIS data also showed that the display of Nyquist plots, and hence the mechanism of corrosion, depended on the acid concentration. In 0.005, 0.010 and 0.050 M concentration, the equivalent circuits $R_s(R_{ct}Q_{dl})$ described the corrosion systems. However, at concentrations $\geq$ 0.100 M, the equivalent circuit $R_s(Q_{dl}[R_{ct}(R_rQ_r)])$ by two time constants was applicable.

Keywords: Solution concentration, Stainless steel, Passive film, Mott–Schottky.

1. Introduction

Stainless steels (especially austenitic types) have many properties such as mechanical strength, chemical resistance, hardness, surface finish, cleanliness and neatness, making them a highly valuable material for many industrial applications. These alloys are the most common multi-component construction materials used by the chemical and petrochemical industries[1-5].

The higher corrosion resistance of stainless steel is due to the presence of a very thin passivating and self-renewable protective layer (passive films) formed on the surface. Generally, the passive films of metals are mainly made up of metallic oxides or hydroxides envisaged as semiconductors. Consequently, semiconducting properties are often observed on the surfaces of the passivity metals[6-9].

Their electrical properties are expected to be crucially important in understanding the protective characters against corrosion. Mott–Schottky analysis has been widely used to study and characterize the semiconducting properties of the passive films, such as the passive films on chromium[10], nickel[11], aluminum[12], cobalt[13], titanium[14,15], steels[16,17] and stainless steels[18,19]. Passivity of stainless steel is usually attributed to the formation on the metal surface of a mixture of iron and chromium oxide film with the semiconducting behavior. In the last decade, the growing research addressing the electronic properties of passive films formed on stainless steels has given an important contribution to the understanding of the corrosion behavior of these alloys[20-23].

The film composition, however, varies with both the alloy composition and the pH of the solution used for film formation, and this is expected to affect the semiconducting properties of the passive film[24,25]. The main effect of increasing pH on film formation is a thickening of the passive film, basically because iron oxides are more stable in alkaline solutions. Thus, for passive films formed on Fe–Cr alloys in alkaline medium, an increase of the amount of Fe(III) oxide has been found by Haupt and Strehblow[26]. Conversely, in acid solutions, a chromium-rich oxide film is formed due to slower dissolution of chromium oxide when compared to iron oxide. Passive films formed in 0.5 M H_2SO_4 on Fe–22Cr single crystal have been described as a bilayer, with a mixed Cr(III) and Fe(III) oxide inner layer being enriched with Cr_2O_3 and a Cr-hydroxide outer layer[27].

However, there are few systematic studies on the effects of solution concentration on the passive behaviour of stainless steel in acidic solutions. The aim of this paper was to investigate the influence of solution concentration on the passive films formed on AISI 321 under OCP conditions using the potentiodynamic polarization and EIS. Also, Mott-Schottky analysis of AISI 321 was performed and the

Corresponding author:
Tel: +98 916 1620892   Fax: +98 811 8257400
Email: a.fattah@basu.ac.ir
Address: Faculty of Engineering, Bu-Ali Sina University, Hamedan 65178-38695, Iran
1. Assistant Professor
2. M.Sc. Student
3. M.Sc. Student

defects concentrations were calculated as a function of solution concentration. The relationship between the defects concentrations and solution concentration has been discussed in order to understand the property of the passivation of AISI 321.

2. Experimental procedures
2.1. Material and test solution

Specimens were fabricated from AISI 321 with the chemical composition (%, wt.): 17.4 Cr, 9.1 Ni, 1.01 Mn, 0.39 Mo, 0.45 Si, 0.39 Ti, 0.013 Al, 0.37 Cu, 0.13 Co, 0.017 Nb, 0.002 V, 0.003 S, 0.05 C. All samples were polished mechanically by abrading with wet emery paper up to 1200 grit size on all sides and then embedded in cold curing epoxy resin. After this, the stainless steels were degreased with acetone, rinsed with distilled water and dried with a stream of air just before immersion. Aerated acidic solutions with six different concentrations were used and the compositions were 0.005, 0.010, 0.050, 0.100, 0.500 and 1.000 M H_2SO_4, respectively. All solutions were made from analytical grade 97% H_2SO_4 and distilled water, and the tests were carried out at ambient temperature.

2.2. Experimental methods

All electrochemical measurements were performed in a conventional three-electrode cell under aerated conditions. The counter electrode was a Pt plate, and all potentials were measured against Ag/AgCl in saturated KCl. All electrochemical measurements were obtained using μautolab potentiostat/galvanostat controlled by a personal computer.

Prior to all electrochemical measurements, working electrodes were immersed at OCP for 1 h to form a steady-state passive film. Potentiodynamic polarization curves were measured potentiodynamically at a scan rate of 1 mV/s starting from -0.25 V (vs. E_{corr}) to 1.1 V. The impedance spectra were measured in a frequency range of 100 kHz –10 mHz at an AC amplitude of 10 mV (rms). The validation of the impedance spectra was done by checking the linearity condition, i.e. measuring spectra at AC signal amplitudes between 5 and 15 mV (rms). Each electrochemical measurement was repeated at least three times. For EIS data modeling and curve-fitting method, NOVA impedance software was used. Mott-Schottky analysis was carried out on the passive films at a frequency of 1 kHz using a 10 mV ac signal and a step rate of 25 mV in the cathodic direction.

3. Results and discussion
3.1. Potentiodynamic polarization

Figure 1 shows the potentiodynamic polarization curves of AISI 321 in 0.005, 0.010, 0.050, 0.100, 0.500 and 1.000 M H_2SO_4. By comparing the polarization curves in different solution, the corrosion potentials were found to shift slightly towards positive direction with an increase in solution concentration. For all curves, the current was increased with the potential during the early stage of passivation and no obvious current peak was observed. It can be found that the passive currents were increased with solution concentration. Also, all curves exhibited similar features, with a passive potential range extending from the corrosion potential to the onset of transpassivity.
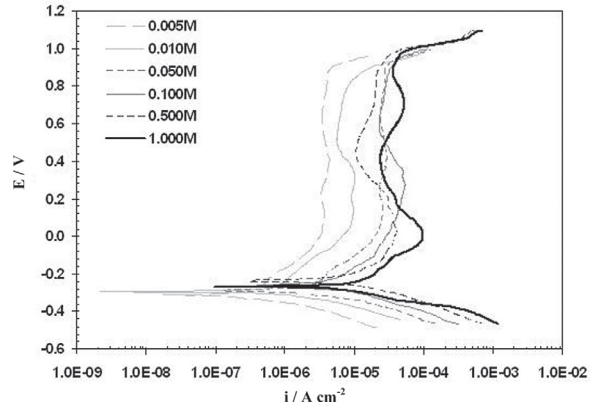

Fig. 1. Potentiodynamic polarization curves at 1 mV/s for AISI 321 in H_2SO_4 solutions with different concentrations.

3.2. Mott-Schottky analysis

The previous study[28-30] has proved that the outer layer of passive films contained the space charge layer and sustained a potential drop across the film. The charge distribution at the semiconductor/solution is usually determined based on Mott-Schottky relationship by measuring electrode capacitance, C, as a function of electrode potential E[28-30]:

$$\frac{1}{C^2} = \frac{2}{\varepsilon \varepsilon_0 e N_D}\left(E - E_{FB} - \frac{kT}{e}\right) \quad \text{for n-type semiconductor} \quad (1)$$

$$\frac{1}{C^2} = -\frac{2}{\varepsilon \varepsilon_0 e N_A}\left(E - E_{FB} - \frac{kT}{e}\right) \text{for p-type semiconductor} \quad (2)$$

where e is the electron charge (-1.602×10^{-19} C), N_D is the donor density for n–type semiconductor (cm^{-3}), N_A is the acceptor density for p–type semiconductor (cm^{-3}), ε is the dielectric constant of the passive film, usually taken as 15.6[31-34], ε_0 is the vacuum permittivity (8.854×10^{-14} F cm^{-1}), k is the Boltzmann constant (1.38×10^{-23} J K^{-1}), T is the absolute temperature and E_{FB} is the flat band potential. From Eq. (1), N_D can be determined from the slope of the experimental C^{-2} versus E plots, and E_{FB} from the extrapolation of the linear portion to $C^{-2} = 0$.

Figure 2 shows the Mott-Schottky plots of AISI 321 in 0.005, 0.010, 0.050, 0.100, 0.500 and 1.000 M H_2SO_4. First, it should be noted that for all concentrations, capacitances were clearly increased with solution concentration. Second, all plots showed three regions in which a linear relationship between C^{-2} and E could be observed. The negative slopes in region I can be attributed to a p-type behaviour, probably due to the presence of Cr_2O_3, FeO and NiO on the passive films[35]. Region II presented positive slopes, depicting an n-type semiconducting behaviour. Finally, the negative slopes in region III can be attributed to p-type behaviour, with a peak at around 0.6 V. This feature is usually explained in terms of a strong dependence of the Faradaic current on potential in the transpaasive region[35]. In this sense, the behaviour of capacitance at high potentials near the transpaasive region may be attributed to the development of an inversion layer as a result of an increasing concentration in the valence band (high valency Cr in the film prior to transpaasive dissolution).

In all plots, straight lines with a negative and positive slope were separated by a narrow potential plateau region (0.0 to 0.05 V), where the flat band potential (E_{fb}) was observed. In the potential more than 0.0 V, the positive slope indicated n-type behavior and in the potential less than 0.0 V, the negative slope was representative of the behavior of a p-type behavior. Thus, Mott-Schottky analysis showed that the passive films formed on this stainless steel behaved as n-type and p-type semiconductors above and below the flat band potential, respectively. This behavior implies that the passive films could have a duplex structure, which would not have been realized if the measurements were restricted to only the more anodic potentials. Early

studies of the bipolar duplex structures of passive films on stainless steels are attributed to Sato[36], and since then, other investigations have given credence to this observation[37,38]. It is widely accepted that the inner part of the passive film, which has a p-type behavior, consists mainly of Cr oxides, whereas the outer region, with the features of an n-type behavior, is predominantly Fe oxides. Contributions to the p-type behavior at $E < E_{fb}$ are restricted to the inner Cr oxide layer, with negligible contributions from the Fe oxides in the outer part of the film, whereas the n-type behavior at $E > E_{fb}$ depends exclusively on the outer Fe oxide region with no contribution from the Cr oxide region[38].

According to Eq. (1), donor density has been determined from the positive slopes in region II of Figure 2. Also, acceptor density has been calculated from the negative slopes in region III of Figure 2, according to Eq. (2). Figures 3(a) and (b) show the calculated donor and acceptor densities for the films formed on AISI 321 in 0.005, 0.010, 0.050, 0.100, 0.500 and 1.000 M H_2SO_4. The orders of magnitude were around 10^{21} cm^{-3}, comparable to those reported in other studies[38]. According to Figures 3(a) and (b), the donor and acceptor densities were increased with solution concentration, respectively. Changes in donor and acceptor densities corresponded to the non-stoichiometry defects in the passive film. Therefore, it can be concluded that the passive film on AISI 321 is disordered, becoming more visible at the higher concentration. Based on Point defect model (PDM), the donors or acceptors in semiconducting passive layers are point defects, as explained briefly in the part 3.3.
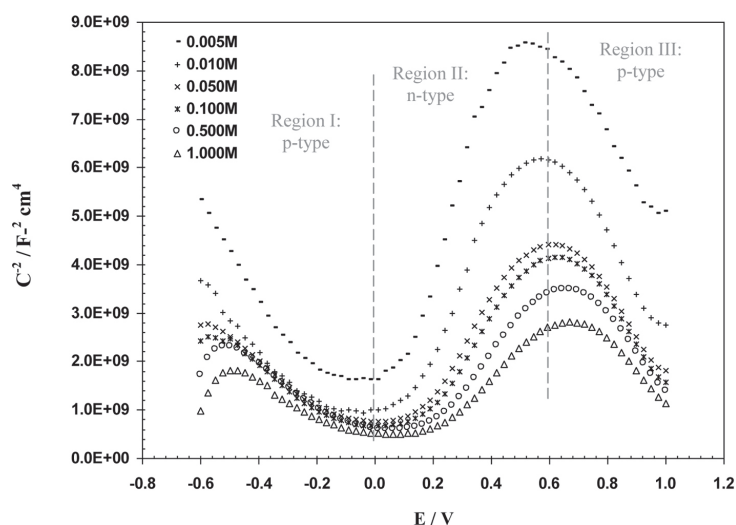

Fig. 2. Mott-Schottky plots of the passive films formed on AISI 321 in H_2SO_4 solutions. The electrodes were immersed at OCP for 1 h to form a steady-state passive film.
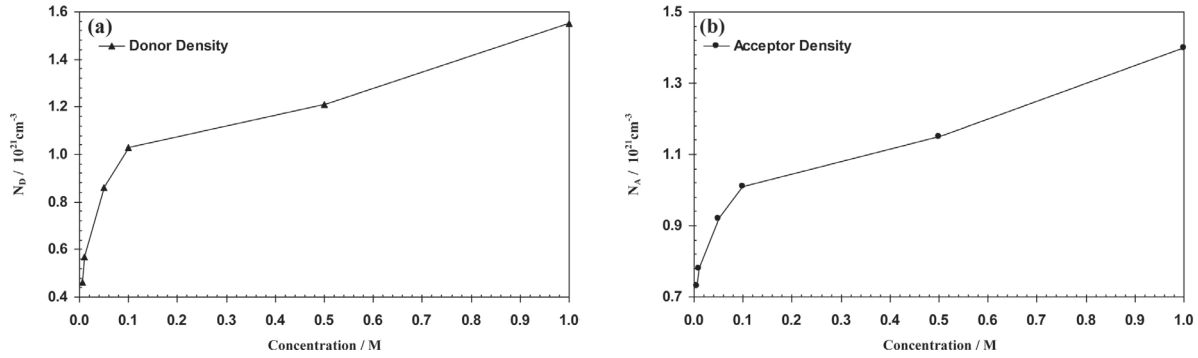
Fig. 3. (a) Donor and (b) acceptor densities of the passive films formed on AISI 321 in sulfuric acid solutions as a function of concentration.

3.3. Point defect model

Although many models and theories have been proposed to explain the passivation of materials, there is still a lack of a satisfactory description of the phenomenon. The PDM, which was developed by Chao, Lin and Macdonald[39-41], described the growth and breakdown of passive film qualitatively from a microscopic perspective. This model is based on the assumption that the passive film contains a high concentration of point defects, such as oxygen vacancies and metal cation vacancies. The growth and breakdown of the passive film involves the migration of these point defects under the influence of the electrostatic field in the film. Thus, the key parameter in determining the transport of point defects and hence, the kinetics of film growth is the density of the defects in film. The PDM[42,43] postulates that passive films are bilayer structures comprising a highly defective barrier layer that grows into the metal and an outer layer formed via the hydrolysis of cations transmitted through the barrier layer and the subsequent precipitation of a hydroxide, oxyhydroxide, or oxide, depending upon the formation conditions. The outer layer may also be formed by transformation of the outer surface of the barrier layer itself, provided that the outer layer is thermodynamically more stable than the barrier layer.

The PDM further postulates that the point defects present in a barrier layer are, in general, cation vacancies ($V_M^{\chi'}$), oxygen vacancies ($V_O^{\cdot\cdot}$), and cation interstitials ($M_i^{\chi+}$), as designated by the Kroger-Vink notation. The defect structure of the barrier layer can be understood in terms of the set of defect generation and annihilation reactions occurring at the metal/barrier layer interface and at the barrier layer-solution interface, as depicted in Figure 4[42,43].
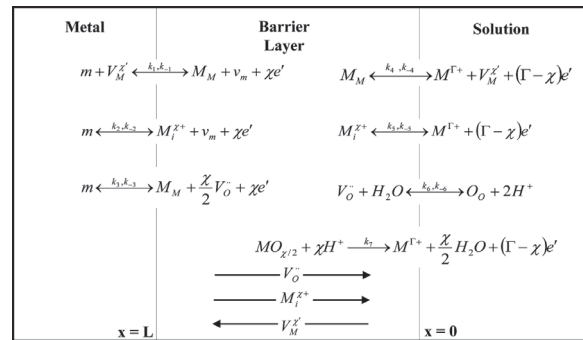

Fig. 4. Interfacial defect generation-annihilation reactions postulated to occur in the growth of passive films according to the PDM. m = metal atom, M_M = metal cation on the metal sublattice, O_O= oxygen anion on the oxygen sublattice, and $M^{\Gamma+}$= metal cation in solution[42,43].

Cation vacancies are electron acceptors, thereby doping the barrier layer p-type, whereas oxygen vacancies and metal interstitials are electron donors, resulting in n-type doping. Thus, on pure metals, the barrier layer is essentially a highly doped, defect semiconductor, as demonstrated by Mott-Schottky analysis. Not unexpectedly, the situation with regard to alloys is somewhat more complicated than that for the pure metals, because substitution of other metal cations having oxidation states different from the host on the cation sublattice may also impact the electronic defect structure of the film. Thus, while the barrier layers on pure chromium and Fe-Cr-Ni alloys are commonly described as being "defective Cr_2O_3," the one on pure chromium is normally p-type in electronic character, while those on the stainless steels are n-type. It is not known whether this difference is due to doping of the barrier layer by other alloying elements (Ni, Fe), as indicated above, or it can be because of the

inhibition of cation vacancy generation relative to the generation of oxygen vacancies and metal interstitials in the barrier layer on the alloys compared with that on pure chromium[42,43].

According to the PDM, the flux of oxygen vacancy and/or cation interstitials (Cr^{2+}, Cr^{3+}, Fe^{2+}, and Ni^{2+}) through the passive film is essential to the film growth process. In this concept, the dominant point defects in the passive film at low potential passive region are considered to be oxygen vacancies and/or cation interstitials acting as electron donors.

3.4. EIS measurements

Figures 5(a) and (b) present the EIS spectra (Nyquist plots) obtained for the AISI 321 at the OCP after 1 h immersion in H_2SO_4 solutions. In Figure 5(a), the Nyquist plots display one capacitive loop (one time-constant), indicating that only one reaction controls the corrosion process. This reaction is the homogeneous corrosion of the surface in contact with the solution. In Figure 5(b), all Nyquist plots have the same shape where a semicircle covers most of the high-frequency region and a capacitive arc in the low-frequency domain (which appears at frequency ≤ 0.04 Hz, except 0.100 M).

Hermas and Morad[5] have reported that the high-frequency semicircles are generally associated with the charge transfer at the electrode/ solution interface, i.e. an electrical double layer, and their diameters indicate how resistant the interface is against the charge transfer and the capacitive arc reflects the relaxation of adsorbed intermediates. These intermediates include [FeOH]ads and [FeH]ads. It was pointed out that in strong acidic solution and in the potential region near the OCP, both the anodic iron dissolution and the hydrogen evolution occurred simultaneously on the electrode surface. The appearance of the capacitive arc indicated that the kinetics of the dissolution of the surface oxide film was limited by diffusion of the oxidation products.

The equivalent circuit used for analyzing and fitting the impedance data by one time constant (Figure 5(a)) is shown in Figure 6. This equivalent circuit is composed by one time constant, as proposed by Pardo et al.[44], and used to describe the behaviour of AISI 304 and 316 stainless steels in H_2SO_4 solutions.
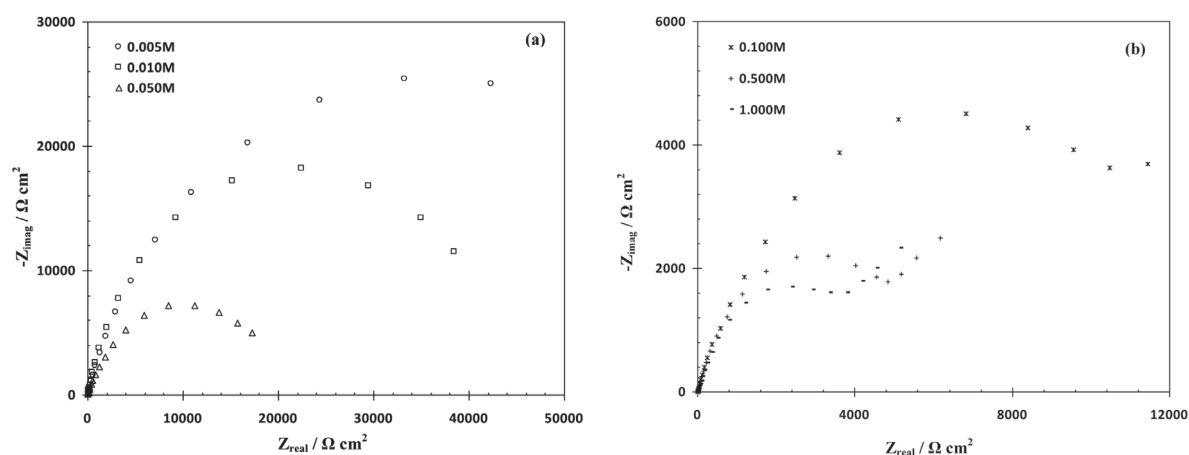

Fig. 5. Nyquist plots of AISI 321 in (a) 0.005, 0.010 and 0.050 M H_2SO_4, and (b) 0.100, 0.500 and 1.000 M H_2SO_4. The electrodes were immersed at OCP for 1 h.
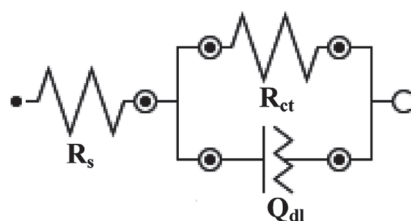

Fig. 6. The best equivalent circuit tested to model the experimental EIS data with one time constant.

In this circuit, as shown in Figure 6, R_s is in a series with a parallel combination of Q_{dl} (double layer constant phase element) and R_{ct} (charge transfer resistance). Q_{dl} is used instead of pure capacitance to account for the depression of the capacitive loop which is usually attributed to surface heterogeneity. The impedance of the constant phase element (Q) is presented by

$$Z_Q = \left[Y_0 (j\omega)^n \right]^{-1} \qquad (3)$$

where n is associated with the roughness of the electrode surface and Y_0 is a frequency-independent real constant representing the total capacitance of the Q. When n = 1, it means that Q is equivalent to a pure capacitor and $Y_0 = C$[45]. As shown in Figure 7, this model could fit the impedance data obtained at concentrations ≤ 0.050 M.
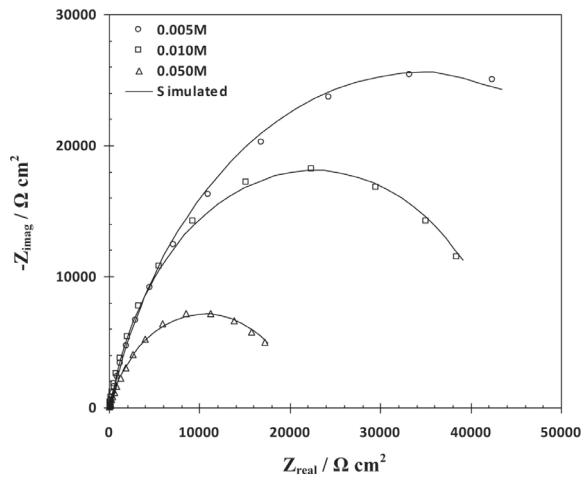

Fig. 7. The fitting results of typical Nyquist plots of AISI 321 in 0.005, 0.010 and 0.050 M H_2SO_4.

Table 1 presents the best fitting parameters obtained for the films formed on AISI 321 immersed in 0.005, 0.010 and 0.050 M H_2SO_4 solutions. As shown in Table 1, the fitting parameters R_{ct} and Y_{0dl} are affected by solution concentration. R_{ct} suffers decrease, and the admittance of Q_{dl} seems to be very close to the values expected for a double layer capacitance.

Table 1. Best fitting parameters for the impedance spectra of AISI 321 in 0.005, 0.010 and 0.050 M H_2SO_4

Solution (M)	R_s (Ω cm²)	R_{ct} (kΩ cm²)	Y_{0dl} (μF cm⁻² sⁿ⁻¹)	n_{dl}
0.005	92.92	69.102	94.39	0.813
0.010	63.49	45.246	75.56	0.859
0.050	14.13	19.668	122.64	0.801

The other equivalent circuit used for analyzing and fitting the impedance data by the two time constants (Figure 5(b)) is shown in Figure 8. This equivalent circuit has been reported to be excellent for modeling the passivation of stainless steels in acidic media[35,46].
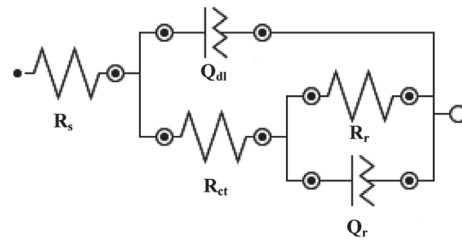

Fig. 8. The best equivalent circuit tested to model the experimental EIS data with two hierarchically distributed time constants.

This circuit presents two time constants. The interpretation suggested for the circuit elements is the following one: the high frequencies (R_{ct}: charge transfer resistance, Q_{dl}: double layer constant phase element) time constant can be associated with the charge transfer process and the low frequencies (R_r, Q_r) time constant can be correlated with the redox processes taking place in the surface film. This equivalent circuit provided the best fitting for the impedance data obtained at concentrations ≥ 0.100 M as shown in Figure 9. Table 2 presents the best fitting parameters obtained for the films formed on AISI 321 immersed in 0.100, 0.500 and 1.000 M H_2SO_4 solutions. Concerning the evolution with solution concentration, the fitting parameters R_{ct} and Y_{0dl} for the films formed on AISI 321 were affected. R_{ct} suffers decrease, and the admittance of Q_{dl} seems to

Table 2. Best fitting parameters for the impedance spectra of AISI 321 in 0.100, 0.500 and 1.000 M H_2SO_4

Solution (M)	R_s (Ω cm²)	R_{ct} (kΩ cm²)	Y_{0dl} (μF cm⁻² sⁿ⁻¹)	n_{dl}	R_r (kΩ cm²)	Y_{0r} (μF cm⁻² sⁿ⁻¹)	n_r
0.100	8.85	12.691	136.24	0.791	9.77	768.73	0.991
0.500	4.41	5.624	130.13	0.823	7.71	4245.52	0.905
1.000	2.52	4.713	205.91	0.775	6.37	4339.16	0.884

be very close to the values expected for a double layer capacitance. Also, the fitting parameters R_r and Y_{0r} are affected by solution concentration. R_r decreases with a tendency to increase with solution concentration, whereas Y_{0r} increases.

As the corrosion rate is inversely proportional to R_{ct}, values of log $(1/R_{ct})$ were plotted as a function of solution concentration (Arrhenius plots) in Figure 10. The corrosion mechanism of the acid dissolution of stainless steel is dependent not only on the hydrogen ion concentration, but also on the counter ion of the acid. It is suggested that the extent of adsorption of SO_4^{2-} ion on the electrode greatly determines the corrosion rate. It was reported[5] that SO_4^{2-} had a low tendency to be adsorbed on the steel surface. Hence, the concentration of surface complex formed is not sufficient to cover the electrode surface from the solution or the complex is not stable enough to be desorbed from the surface.
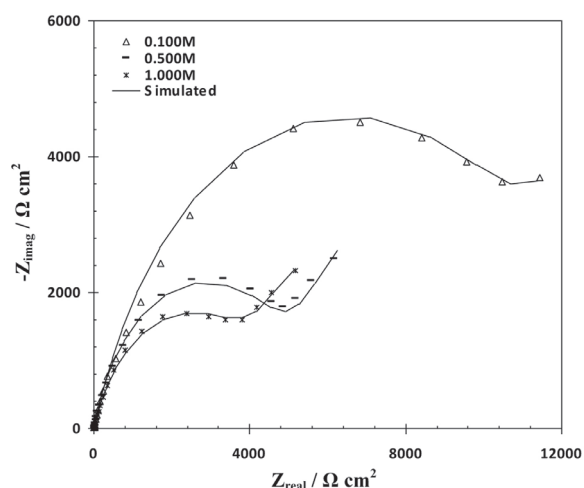

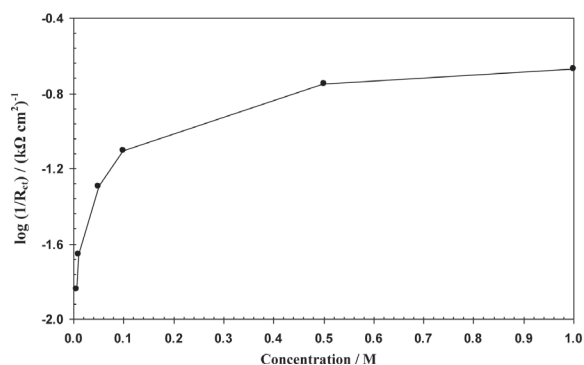*Fig. 9. The fitting results of Nyquist plots of AISI 321 in 0.100, 0.500 and 1.000 M H_2SO_4.*

Fig. 10. Arrhenius plots deduced from the values of R_{ct} obtained for the corrosion of AISI 321 in sulfuric acid solutions.

4. Conclusions

The semiconductor properties of passive films formed on AISI 321 in H_2SO_4 solutions under OCP conditions were investigated in the present work. Conclusions drawn from the study are as follows

1. The polarization curves suggested that AISI 321 showed comparable passive behaviour in sulfuric solutions.
2. By comparing the polarization curves in different solutions, the corrosion potentials were found to shift slightly towards positive direction with an increase in solution concentration. Also, the current was increased wit the potential during the early stage of passivation and no obvious current peak was observed.
3. Mott–Schottky analysis revealed that the existence of a duplex passive film structure composed of two oxide layers of distinct semiconductivities (n-type and p-type).
4. Based on the Mott–Schottky analysis, it was shown that donor and acceptor densities were in the range of 10^{21} cm^{-3} and increased with solution concentration.
5. EIS data showed that the display of Nyquist plots, and hence the mechanism of corrosion, depended on the acid concentration. In 0.005, 0.010 and 0.050 M concentration, the equivalent circuits $R_s(R_{ct}Q_{dl})$ described the corrosion behaviour. At concentrations $\geq$ 0.100 M, the equivalent circuit $R_s(Q_{dl}[R_{ct}(R_rQ_r)])$ was applicable.

References

[1] T. Yamamoto, K. Fushimi, M. Seo, S. Tsuri, T. Adachi and H. Habazaki: Corros. Sci., 51(2009), 1545.
[2] A. Pardo, M.C. Merino, A.E. Coy, F. Viejo, M. Carboneras and R. Arrabal: Acta Mater., 55(2007), 2239.
[3] Y.Y. Chen, Y.M. Liou and H.C. Shih: Mater. Sci. Eng. A, 407(2005), 114.
[4] Z. Shi, G. Song, C.-N. Cao, H. Lin and M. Lu: Electrochim. Acta, 52(2007), 2123.
[5] A.A. Hermas and M.S. Morad: Corros. Sci., 50(2008), 2710.
[6] N.E. Hakiki, M. Da Cunha Belo, A.M.P. Simões and M.G.S. Ferreira: J. Electrochem. Soc., 145(1998), 3821.
[7] M. Da Cunha Belo, N.E. Hakiki and M.G.S. Ferreira: Electrochim. Acta, 44(1999), 2473.
[8] K. Sugimoto and Y. Sawada: Corros. Sci., 17(1997), 425.
[9] M.F. Montemor, A.M.P. Simões, M.G.S. Ferreira and M. Da Cunha Belo: Corros. Sci., 41(1999), 17.
[10] D.-S. Kong, S.-H. Chen, C. Wang and W. Yang: Corros. Sci., 45(2003), 747.
[11] E. Sikora and D.D. Macdonald: Electrochim. Acta, 48(2002), 69.
[12] F.J. Martin, G.T. Cheek, W.E.O. Grady and P.M. Natishan: Corros. Sci., 47(2005), 3187.

[13] M. Pontinha, S. Faty, M.G. Walls, M.G.S. Ferreira and M. Da Cunha Belo: Corros. Sci., 48(2006), 2971.
[14] A.M. Schmidt, D.S. Azambuja and E.M.A. Martini: Corros. Sci., 48(2006), 2901.
[15] K. Azumi and M. Seo: Corros. Sci., 43(2001), 533.
[16] S. Fujimoto and H. Tsuchiya: Corros. Sci., 49(2007), 195.
[17] J. Wielant, V. Goossens, R. Hausbrand and H. Terryn: Electrochim. Acta, 52(2007), 7617.
[18] J. Amri, T. Souier, B. Malki and B. Baroux: Corros. Sci., 50(2008), 431.
[19] S. Ningshen, U. K. Mudali, V.K. Mittal and H.S. Khatak: Corros. Sci., 49(2007), 481.
[20] A.M.P. Simões, M.G.S. Ferreira, B. Rondot and M. da Cunha Belo: J. Electrochem. Soc., 137(1990), 82.
[21] I. Olefjord and L. Wegrelius: Corros. Sci., 31(1990), 89.
[22] S. Mischler, A. Vogel, H. Mathieu and D. Landolt: Corros. Sci., 32(1991), 925.
[23] M.F. Montemor, M.G.S. Ferreira, N.E. Hakiki and M. Da Cunha Belo: Corros. Sci., 42(2000), 1635.
[24] C. Sunseri, S. Piazza and F. Di Quarto: J. Electrochem. Soc., 137(1990), 2411.
[25] M.J. Carmezim, A.M. Simões, M.O. Figueiredo and M. Da Cunha Belo: Corros. Sci., 44(2002), 451.
[26] S. Haupt and H.-H. Strehblow: Corros. Sci., 37(1995), 43.
[27] M.V. Cardoso, S.T. Amaral and E.M.A. Martini: Corros. Sci., 50(2008), 2429.
[28] R.S. Dutta, G.K. Dey and P.K. De: Corros. Sci., 48(2006), 2711.
[29] E.M.A. Martini and I.L. Muller: Corros. Sci., 42(2000), 443.
[30] J. Macak, P. Sajdl, P. Kucera, R. Novotny and J. Vosta: Electrochim. Acta, 51(2006), 3566.
[31] Y.X. Qiao, Y.G. Zheng, W. Ke and P.C. Okafor: Corros. Sci., 51(2009), 979.
[32] Y. Yang, L.-j. Guo and H. Liu: J. Power Sources, 195(2010), 5651.
[33] Y.F. Cheng, C. Yang and J.L. Luo: Thin Solid Films, 416(2002), 169.
[34] N. Li, Y. Li, S. Wang and F. Wang: Electrochim. Acta, 52(2006), 760.
[35] C. Escrivà-Cerdán, E. Blasco-Tamarit, D.M. García-García, J. García-Antóna and A. Guenbour: Electrochim. Acta, 80(2012), 248.
[36] N. Sato: Corros. Sci., 31(1990), 1.
[37] M.G.S. Ferreira, N.E. Hakiki, G. Goodlet, S. Faty, A.M.P. Simões and M. Da Cunha Belo: Electrochim. Acta, 46(2001), 3767.
[38] E.E. Oguzie, J. Li, Y. Liu, D. Chen, Y. Li, K. Yang and F. Wang: Electrochim. Acta, 55(2010), 5028.
[39] C.Y. Chao, L.F. Lin and D.D. Macdonald: J. Electrochem. Soc., 128(1981), 1187.
[40] C.Y. Chao, L.F. Lin and D.D. Macdonald: J. Electrochem. Soc., 128(1981), 1194.
[41] C.Y. Chao, L.F. Lin and D.D. Macdonald: J. Electrochem. Soc., 129(1982), 1874.
[42] D.D. Macdonald: J. Electrochem. Soc., 153(2006), 213.
[43] D.D. Macdonald: J. Nucl. Mater., 379(2008), 24.
[44] A. Pardo, M.C. Merino, M. Carboneras, F. Viejo, R. Arrabal and J. Munoz: Corros. Sci., 48(2006), 1075.
[45] H. Ma, X. Cheng, G. Li, S. Chen, Z. Quan, S. Zhao and L. Niu: Corros. Sci., 42(2000), 1669.
[46] M. Metikoš-Hukovic, R. Babic, Z. Grubac, Z. Petrovic and N. Lajçi: Corros. Sci., 53(2011), 2176.